

Unveiling First Order CMR Transitions in the Two-Orbital Model for Manganites

Cengiz Şen,^{1,2} Gonzalo Alvarez,³ and Elbio Dagotto^{1,2}

¹*Department of Physics and Astronomy, The University of Tennessee, Knoxville, TN 37996*

²*Materials Science and Technology Division, Oak Ridge National Laboratory, Oak Ridge, TN 32831*

³*Computer Science & Mathematics Division and Center for Nanophase Materials Sciences,*

Oak Ridge National Laboratory, Oak Ridge, TN 37831

(Dated: May 1, 2022)

Large scale Monte Carlo simulation results for the two-orbital model for manganites, including Jahn-Teller lattice distortions, are here presented. At hole density $x = 1/4$ and in the vicinity of the region of competition between the ferromagnetic metallic and spin-charge-orbital ordered insulating phases, the colossal magnetoresistance (CMR) phenomenon is observed with a magnetoresistance ratio $\sim 10,000\%$. Our main result is that this CMR transition is found to be of first order in some portions of the phase diagram, in agreement with early results from neutron scattering, specific heat, and magnetization, thus solving a notorious discrepancy between experiments and previous theoretical studies. The first-order characteristics of the transition survive, and are actually enhanced, when weak quenched disorder is introduced.

Introduction. The manganese oxides known as manganites continue attracting considerable attention due to the presence of several competing tendencies in their rich phase diagrams, with a variety of spin, charge, and orbital orders [1, 2]. Moreover, these compounds display the famous CMR effect, where the resistivity is drastically reduced by fields of a few Teslas. Early theoretical investigations [3] remarked the importance of phase competition to understand the CMR, which occurs when an insulating state, typically also spin-charge-orbital ordered, is close in energy to the low-energy ferromagnetic (FM) metallic ground state induced by double exchange. These effects were clear in simplified phenomenological models and resistor-network simulations when in the presence of disorder [4]. However, it is important to verify at a more fundamental level if the basic model Hamiltonians that are widely perceived as being realistic for manganites, including double-exchange, superexchange, and lattice distortion tendencies, are indeed compatible with the CMR phenomenology. Recently, our group and others initiated this effort based on Monte Carlo (MC) simulations [5–8]. This is a challenging task since computer efforts based on the exact solution of the fermionic e_g sector, for fixed MC-generated classical t_{2g} spin and lattice configurations, have a CPU time growing as N^4 , with N the number of cluster sites times the number of orbitals. For this reason, recent efforts at realistic electronic densities have used only one e_g orbital, considerably reducing the CPU demands [8]. However, it is clear that the more complete two e_g orbitals model must be investigated for a full understanding of the CMR physics. Alas, since this is far more time consuming, MC results for two orbitals are only scattered in the literature and they have not reached sufficient accuracy to unveil the true properties of this model in the CMR regime.

In addition, an important qualitative difference still persists with regards to the *order* of the CMR transitions. Until now, MC simulations carried out at

CMR realistic hole densities, such as $x = 0.33$ or 0.25 , have indicated the presence of a rapid crossover, yet continuous, transition from the low- T FM metal to the high- T paramagnetic (PM) insulator. This occurs even in the clean limit of the MC simulations, i.e. without quenched disorder. While these results are in agreement with the phenomenology of many CMR manganites [2], there are notorious examples where the CMR transition is of first order, such as for $\text{Pr}_{0.55}(\text{Ca}_{0.75}\text{Sr}_{0.25})_{0.45}\text{MnO}_3$ [9], $\text{Sm}_{0.52}\text{Sr}_{0.48}\text{MnO}_3$ [10, 11], $(\text{Nd}_{0.5}\text{Sm}_{0.5})_{0.55}(\text{Ba}_{0.5}\text{Sr}_{0.5})_{0.45}\text{MnO}_3$ [12], and others. In fact, early experimental studies already reported signs of irreversibility at the CMR transition for one of the most widely studied manganites, $\text{La}_{1-x}\text{Ca}_x\text{MnO}_3$ (LCMO) at $x = 0.33$, suggesting that its transition is weakly first-order [13]. Subsequent magnetization and specific heat analysis clarified that indeed the $x = 0.33$ LCMO transition is of first order [14]. Recent investigations have also addressed the order of the CMR transition, revealing multicritical characteristics in $\text{RE}_{0.55}\text{Sr}_{0.45}\text{MnO}_3$ (RE = Rare-Earth) [15].

Our main goal in this publication is to solve this puzzling theory-experiment disagreement by carrying out a large-scale computational study of the two-orbital model for manganites at $x = 1/4$. It will be shown that our MC data unveils the presence of a first-order CMR FM-PM transition in this realistic model and density.

Model and techniques. The two-orbital model Hamiltonian used here is widely considered the minimal model for the proper description of the electronic properties of manganites and it has been extensively discussed before [16]. For this reason only a schematic description will be here provided. The model is given by $H = H_{\text{DE}} + H_{\text{JT}} + H_{\text{AF}} + H_{\text{Dis}}$ [17]. At every Mn site it contains e_g electrons and t_{2g} localized spins. H_{DE} represents the nearest-neighbors double exchange (DE) e_g electron hopping at infinite Hund coupling. This term favors ferromagnetism away from the electronic density

$n = 1$. H_{JT} is the coupling between fermions and oxygen breathing and Jahn-Teller lattice distortions, with coupling strength λ . The sum $H_{DE} + H_{JT}$ is Eq.(4) of Ref. 7, with the hopping along x for orbital $a = x^2 - y^2$, t_{aa} , as the energy unit. $H_{AF} = J_{AF} \sum_{\langle ij \rangle} \mathbf{S}_i \cdot \mathbf{S}_j$ is the standard nearest-neighbors Heisenberg antiferromagnetic coupling among the (classical) t_{2g} spins. Finally, $H_{Dis} = \sum_i \Delta_i n_i$ is the quenched disorder term, with $\Delta_i = \Delta \times r_i$ ($\Delta =$ disorder strength; $r_i =$ bimodal random number 1 or -1).

Details of the computer simulation. The methodology of our MC simulations, based on the fermionic sector exact diagonalization described before, is standard and readers should consult [2] for details. However, the extensive characteristics of the present MC simulations merits a detailed discussion. The procedure was the following. For the clean-limit results $\Delta = 0$, a random spin and lattice configuration was chosen at the highest studied temperature, $T = 0.33$, to initiate the runs. After 10,000 MC steps, T was reduced and another 10,000 steps were performed. This “cooling down” process continued, using a grid with 23 temperatures (lowest 1/300) that was denser near the critical temperatures T_C . After this already demanding first step, the cooling-down results (obtained by measuring during the last 5,000 MC steps per T) revealed sharp, yet continuous, transitions at all couplings. However, at particular T s in the MC time evolution indications of insufficient convergence were found. Thus, next for each T the results were further refined using additional 10,000 MC steps for extra thermalization, followed by 100,000 MC steps for measurements. By monitoring the results during the final MC evolution it was observed that this large effort produces now fairly stable results, revealing the first-order transitions in the region of phase competition discussed below.

The clean-limit effort needed standard computer clusters with ~ 100 nodes. However, a similar procedure with quenched disorder, requiring 40 r_i disorder configurations, 6 disorder strengths (Δ), and 20 temperatures for each J_{AF} , would have been impossible. Thus, the results with disorder reported below were obtained using the UT-ORNL Kraken supercomputer (Cray XT5), where up to 5,000 processors were employed simultaneously for periods of 24 hours. This amounts to a total computational effort in Figs. 3(c) and 3(d) (see below) of $\sim 250,000$ hours (~ 30 years if ran serially).

Clean limit phase diagram. The clean-limit phase diagram of the two-orbital model is in Fig. 1. The chosen coupling $\lambda = 1.3$ is representative of the regime where metallic and Jahn-Teller distorted insulating phases are in competition. The hole density $x = 1/4$ is in the realistic range of experimental CMR investigations. Varying J_{AF} , and via the MC procedure described before, a systematic analysis of spin and charge correlations (e.g. see Fig. 2) leads to a phase diagram where the FM metallic phase generated by the DE mechanism competes with a previously discussed $C_{0.25}E_{0.75}$ insulator [18] (shown in

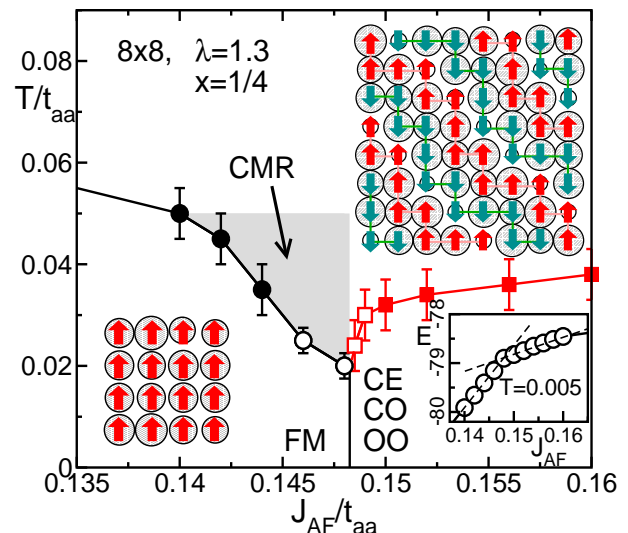


FIG. 1: (Color online) Clean-limit MC phase diagram of the $x = 1/4$ doped two-orbital model at $\lambda = 1.3$ and on an 8×8 lattice. Critical temperatures are estimated from spin structure factors (Fig. 2) and real-space spin-spin correlations (not shown). First (second) order transitions are indicated with open (filled) symbols, and the shaded region is where the CMR is observed (Fig. 3). Also shown are the $T=0$ arrangements of classical spins and electronic charges (magnitude proportional to the radius of the circles) for the competing metallic and insulating states. *Inset:* total energy vs. J_{AF} . The straight lines crossing indicates a low- T first-order transition. The spins were frozen to the FM and CE perfect spin states and the oxygen distortions were MC relaxed.

Fig. 1). This “CE” state is the natural generalization to $x = 1/4$ of the well-known $x = 1/2$ CE state [1–3], and they only differ in the shape of the zigzag chains. Like in all computational based efforts, here relatively small clusters are used, but it is well known that locating the temperature range where the relevant correlation lengths are as large as the cluster size provides qualitatively correct estimations of trends and critical temperatures.

The main novelty of the phase diagram in Fig. 1 is the identification of a first-order transition separating the FM metallic phase from the PM high- T state, in the coupling range close to the competing CE insulator. Previous MC investigations had not reached sufficient accuracy to detect this first-order transition at realistic hole densities, such as $x = 1/4$. While previous efforts had clearly established the first-order nature of the direct low- T FM-CE transition (see inset of Fig. 1), now observing the more subtle first-order FM-PM transition represents qualitative progress in the modeling of manganites.

Figure 2(a) illustrates how the spin structure factor varies with T . At $\mathbf{q}=(0,0)$ and close to the region of CE competition, a discontinuous transition exists between the FM and PM states. There is also a first-order transition from the CE to the PM state, close to the FM region. our new results reveal that the true phase diagram of clean-limit manganite models actually has “multicrit-

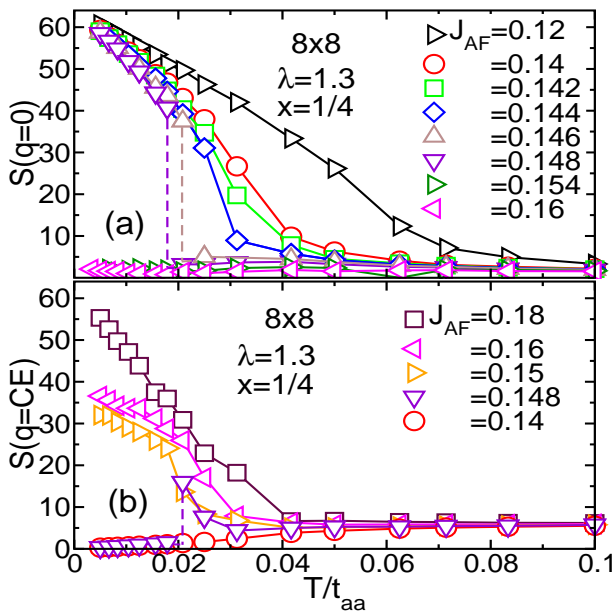


FIG. 2: (Color online) Spin structure factor ($S(\mathbf{q})$) vs. T for the momenta corresponding to the (a) FM and (b) CE states. $S(\mathbf{q})$ was used to determine the critical temperatures in Fig 1. For the CE phase, the relevant momenta are $\mathbf{q}=(\pi/4, 3\pi/4)$, $(\pi/2, \pi/2)$, and $(3\pi/4, \pi/4)$, as well as $\mathbf{q}'=\mathbf{q}+\pi$ (i.e. rotating the zigzag chains by 90-degrees).

ical” characteristics, with the robust FM-CE first-order transition at low T splitting into still first-order FM-PM and CE-PM transitions with increasing T , each ending at critical points (whose precise location is beyond our accuracy). These results are compatible with recent multicritical characteristics revealed in some manganites [15].

CMR effect. The first-order nature of the transitions observed here dramatically affects the transport properties. Using the standard Kubo formula to calculate conductances [5, 7], Fig. 3 shows the resistivity (ρ) vs. T obtained in our simulations. Fig. 3(a) are results in the clean limit, varying J_{AF} in the region of FM-CE competition. At couplings such as $J_{AF}=0.148$, ρ is insulating upon cooling, closely following results for $J_{AF}=0.16$ with a CE ground state. However, at the FM transition $T_C \sim 0.02$ (~ 100 K, if $t_{aa}=0.5$ eV), ρ becomes metallic via an abrupt discontinuity, in excellent agreement with several experiments [9–14]. As T_C increases, moving the system further away from the CE state, the transition becomes continuous and at $J_{AF}=0.12$ the FM transition is barely noticeable in the slope of ρ vs. T . For completeness, in Fig. 4(c) results using a 12×12 cluster for only one set of couplings λ - J_{AF} (due to its high CPU cost) are shown, indicating that cluster size effects are small [19].

Figure 3(b) contains the ρ curves in the presence of magnetic fields H . The observed trends are again in excellent agreement with experiments [9–14], with an overall rapid decrease of ρ and with ρ -peak positions moving to higher T with increasing H , and all the curves merging at approximately room T (i.e. $T \sim 0.06$ if $t_{aa} \sim 0.5$ eV).

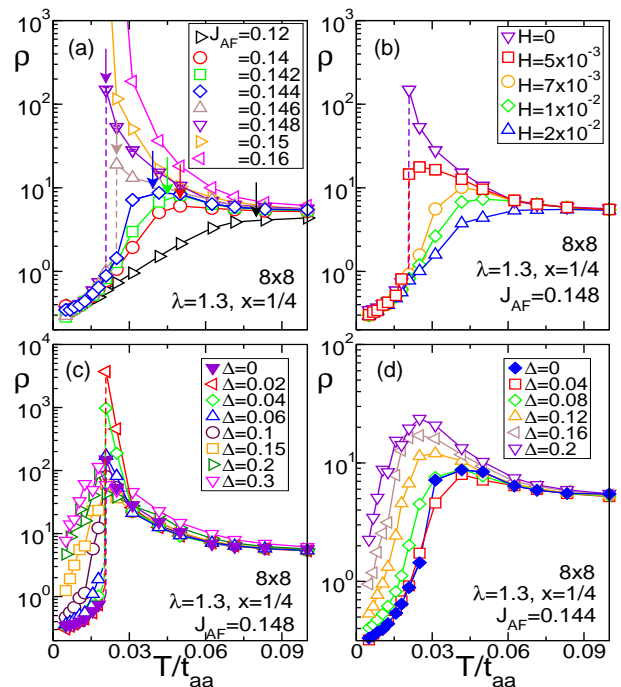


FIG. 3: (Color online) (a) ρ vs. T , illustrating the metal-insulator transition varying J_{AF} . Arrows indicate the magnetic T_C s. Error bars are small (shown only at $J_{AF} = 0.148$). (b) Magnetic field effects (along the z -direction) on the ρ vs. T curves, showing the CMR effect. (c,d) Quenched disorder influence (averages over 40 disorder configurations) on the ρ vs. T curves for (c) $J_{AF}=0.148$ and (d) $J_{AF}=0.144$, with first-order and continuous (but rapid) transitions, respectively.

At a small field $H = 7 \times 10^{-3} t_{aa}$, the magnetoresistance $(\rho(0) - \rho(H))/\rho(H) \times 100\%$ is $\sim 10,000\%$ also in good agreement with CMR phenomenology.

Influence of Quenched Disorder. Experiments and theoretical calculations have shown the importance that quenched disorder has over the CMR effect [2]. It is expected that the clean-limit fine tuning of couplings needed to obtain a CMR (Fig. 1) will be removed once disorder is incorporated. Thus, it is important to analyze the influence of disorder on our results. Using the on-site quenched disorder form described before, results are in Figs. 3(c,d). Panel (c) illustrates how the clean-limit first-order transition is eventually rendered continuous by increasing the disorder strength. However, the discontinuity in ρ first increases with increasing Δ before it is reduced. This result is compatible with the observed multicritical behavior even with disorder [15]. Also as in experiments, when the clean-limit transition is second order, quenched disorder decreases the T where the peak occurs while increasing ρ (panel (d)).

The CMR effect observed in our clean-limit MC simulations can be understood qualitatively via measurements of a variety of observables, similarly as in previous investigations [8]. For instance, Fig. 4(a) contains the spin and charge structure factors, $S(\mathbf{q})$ and $n(\mathbf{q})$, at the momenta of relevance for the CE phase, but in the CMR regime

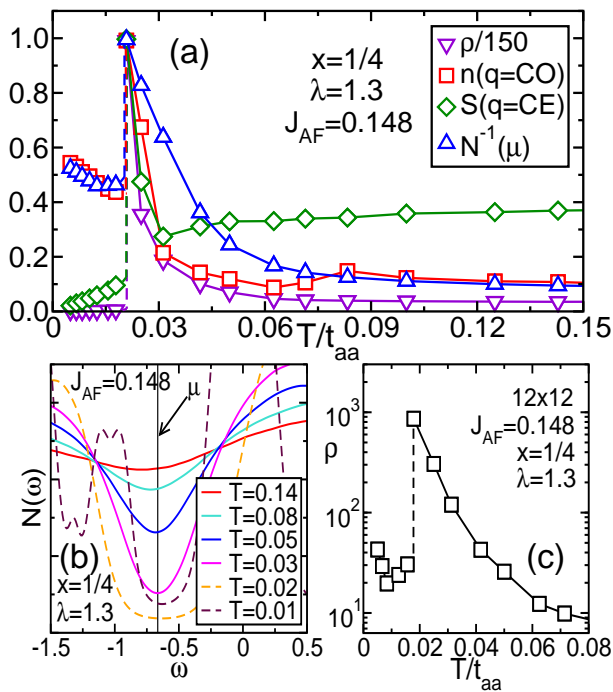


FIG. 4: (Color online) (a) Spin $S(\mathbf{q})$ and charge $n(\mathbf{q})$ structure factors, shown together with the resistivity ρ and the Fermi-level inverse density-of-states, vs. T . The “ $\mathbf{q}=\text{CO}$ ” shorthand stands for the characteristic momenta of the CE state ($\mathbf{q}=(\pi/2, \pi/2)$, (π, π) , and $(3\pi/2, 3\pi/2)$), and momenta obtained by rotating the zigzag chains by $\pi/2$). $n(\mathbf{q})$ is obtained by Fourier-transforming the quantum correlations between local charge densities among e_g orbitals $x^2 - y^2$ and $3z^2 - r^2$, and averaging over the MC steps. (b) Pseudogap in the density of states $N(\omega)$ as T is reduced. (c) ρ vs. T for a 12×12 cluster, showing also a first-order transition.

where the $T = 0$ ground state is FM. As T decreases, not only ρ rapidly increases but so do $S(\mathbf{q}_{CE})$ and $n(\mathbf{q}_{CO})$, showing that the system behaves as if the ground state were CE, developing robust CE short-range correlations. However, at T_C an abrupt transition occurs to the true FM ground state. This switch from CE-dominated to FM-dominated characteristics with cooling may occur if the high- T short-range-ordered CE state has a high entropy. Note also that at low- T , the charge correlations in the FM state are still robust at short distances. Finally, also note that at a $T^*/t_{aa} \sim 0.07 - 0.08$, considerably higher than T_C , the CE tendencies start developing upon cooling [20], and this occurs concomitantly with the presence of a density-of-states pseudogap (Fig. 4(b)), as also observed in photoemission experiments [21]. It is gratifying to observe similar results above T_C for both the present model and the model studied in Ref. 8. Finally, note that the many observations of FM signals above T_C in several manganites [2] are not incompatible with the clean-limit Fig. 4 since quenched disorder is known to increase the strength of the FM component.

Conclusions. The observation of first-order CMR transitions in models for manganites was here reported, solv-

ing a notorious theory-experiment discrepancy. A large-scale computer simulation was needed to reach our conclusions. Robust CMR ratios were found, as well as a CMR state above T_C with short range CE characteristics. Weak quenched disorder preserves the first-order transitions, as in recent experiments [15].

Acknowledgment. This work was supported by the NSF grant DMR-0706020 and by the Division of Materials Sciences and Engineering, Office of Basic Energy Sciences, U.S. DOE. The computer simulations were possible in part by a NSF allocation of advanced computing resources at the Kraken (Cray XT5) supercomputer located at the National Institute for Computational Sciences (<http://www.nics.tennessee.edu/>). A portion of this research was conducted at the Center for Nanophase Materials Sciences at ORNL. This research used the SPF software (<http://www.ornl.gov/~gz1/spf/>).

- [1] M. Salamon and M. Jaime, *Rev. Mod. Phys.* **73**, 583 (2001); J. De Teresa *et al.*, *Nature* **386**, 256 (1997); M. Uehara *et al.*, *Nature* **399**, 560 (1999).
- [2] E. Dagotto *et al.*, *Phys. Rep.* **344**, 1 (2001).
- [3] A. Moreo *et al.*, *Science* **283**, 2034 (1999).
- [4] J. Burgý *et al.*, *Phys. Rev. Lett.* **87**, 277202 (2001); *ibid.*, *Phys. Rev. Lett.* **92**, 097202 (2004); M. Mayr *et al.*, *Phys. Rev. Lett.* **86**, 135 (2001).
- [5] J. A. Vergés *et al.*, *Phys. Rev. Lett.* **88**, 136401 (2002).
- [6] S. Kumar and P. Majumdar, *Phys. Rev. Lett.* **96**, 016602 (2006); *ibid.*, *Phys. Rev. Lett.* **96**, 136601 (2005).
- [7] C. Şen *et al.*, *Phys. Rev. B* **73**, 224441 (2006).
- [8] C. Şen *et al.*, *Phys. Rev. Lett.* **98**, 127202 (2007).
- [9] Y. Tomioka and Y. Tokura, *Phys. Rev. B* **66**, 104416 (2002).
- [10] Y. Tomioka *et al.*, *Phys. Rev. B* **74**, 104420 (2006).
- [11] Y. Tomioka *et al.*, *Phys. Rev. B* **80**, 174414 (2009).
- [12] Y. Tomioka and Y. Tokura, *Phys. Rev. B* **70**, 014432 (2004).
- [13] J. W. Lynn *et al.*, *Phys. Rev. Lett.* **76**, 4046 (1996).
- [14] D. Kim *et al.*, *Phys. Rev. Lett.* **89**, 227202 (2002).
- [15] L. Demko *et al.*, *Phys. Rev. Lett.* **101**, 037206 (2008).
- [16] T. Hotta *et al.*, *Phys. Rev. Lett.* **86**, 4922 (2001).
- [17] The Hubbard U effects are mild at large Hund coupling, T. Hotta *et al.*, *Phys. Rev. B* **62**, 9432 (2000).
- [18] T. Hotta *et al.*, *Phys. Rev. Lett.* **90**, 247203 (2003).
- [19] Preliminary results on $4 \times 4 \times 4$ clusters (not shown) suggest that a similar CMR peak is obtained in three dimensions, but the first order transition is smeared by the frustration effect caused by the geometry of the CE $x = 1/4$ zigzag chains that do not fit into 4×4 layers. Simulations on unfrustrated $8 \times 8 \times 8$ clusters are currently impossible, justifying why our present effort has focused on two dimensions. Fortunately, there are no reasons to suspect that two and three dimensions will behave differently with regards to the first-order transition.
- [20] D. N. Argyriou *et al.*, *Phys. Rev. Lett.* **89**, 036401 (2002).
- [21] D. Dessau *et al.*, *Phys. Rev. Lett.* **81**, 192 (1998); A. Moreo *et al.*, *Phys. Rev. Lett.* **83**, 2773 (1999).